A bet-hedging strategy for denitrifying bacteria curtails their release of N_2O

Pawel Lycus[1], Manuel Jesús Soriano-Laguna[2], Morten Kjos[1], David John Richardson[2], Andrew James Gates[2], Daniel Aleksanteri Milligan[1], Åsa Frostegård[1], Linda Bergaust[1*], Lars Reier Bakken[1*]

[1]*Department of Chemistry, Biotechnology and Food Science, Norwegian University of Life Sciences, Christian Magnus Falsens vei 1, 1432 Ås, Norway*

[2]*School of Biological Sciences, University of East Anglia, Norwich Research Park, Norwich, NR4 7TJ, UK*

***Corresponding authors**

Linda Bergaust

linda.bergaust@nmbu.no

+47 67232449

Lars R. Bakken

lars.bakken@nmbu.no

+47 67231830

Classification

Biological sciences: Microbiology

Keywords

Ecophysiology, bet-hedging, denitrification, nitrous oxide

Abstract

When oxygen becomes limiting, denitrifying bacteria must prepare for anaerobic respiration by synthesizing the reductases NAR ($NO_3^-\rightarrow NO_2^-$), NIR ($NO_2^-\rightarrow NO$), NOR ($2NO\rightarrow N_2O$) and NOS ($N_2O\rightarrow N_2$), either *en bloc* or sequentially, to avoid entrapment in anoxia without energy. Minimizing the metabolic burden of this precaution is a plausible fitness trait, and we show that the model denitrifier *Paracoccus denitrificans* achieves this by synthesizing NOS in all cells, while only a minority synthesize NIR. Phenotypic diversification with regards to NIR is ascribed to stochastic initiation of gene transcription, which becomes autocatalytic via NO production. Observed gas kinetics suggest that such *bet-hedging* is widespread among denitrifying bacteria. Moreover, in response to oxygenation, *P. denitrificans* preserves NIR in the poles of non-growing *persister cells*, ready to switch to anaerobic respiration in response to sudden anoxia. Our findings add new dimensions to the regulatory biology of denitrification, and identify novel regulatory traits that decrease N_2O emissions.

Significance

Denitrifying microorganisms reduce nitrate to N_2 via nitrite, NO and N_2O under hypoxic/anoxic conditions. Since these organisms are the main sources and sinks for N_2O in the environment, their regulatory biology controls the emission of this potent greenhouse gas. We demonstrate bet-hedging in *Paracoccus denitrificans* when facing hypoxia: a minority of the cells synthesize NIR+NOR, the N_2O source, while all synthesize NOS, the N_2O sink, hence the population becomes a strong net sink for N_2O. Bet-hedging is prominent below 20°C and data indicate that it is widespread in soil organisms. This

suggests a prominent role of bet hedging in controlling N_2O emissions that can now be tested for in other strains and in natural environments.

\body

Introduction

Denitrifying organisms use nitrogen oxyanions and oxides as terminal electron acceptors to sustain respiration in the absence of oxygen. This plays a key role in the global nitrogen cycle, returning reactive nitrogen from the biosphere to the atmosphere (1). Although the final product of denitrification is harmless N_2, fractions are emitted to the atmosphere as the potent greenhouse gas N_2O. The increasing emission of N_2O over the last decade is primarily due to denitrification, ultimately driven by the anthropogenic escalation of the global nitrogen cycle (2). The concerns over climate forcing and destruction of stratospheric ozone by N_2O (3) have fueled increasing interest in the ecology and physiology of denitrifying organisms, with a strong emphasis on the phenomena that determine their N_2O production.

Denitrifying organisms emit N_2O because it is a free intermediate in the reduction of nitrate to N_2, catalyzed by four enzymes encoded by *nar, nir, nor* and *nos* gene clusters (Fig. *1*). These are widespread among prokaryotes in soils, sediments and biofilms (4), and analyses of bacterial genomes have revealed that ~30% of the genomes containing the *nos* genes lacked genes encoding NIR (NirS or NirK, (5)). Such "truncated denitrifiers" have attracted attention because they are net sinks for N_2O, whereas organisms equipped with NIR, NOR and NOS are both sinks and sources. This was taken to suggest that the abundance of the structural gene, *nosZ*, could predict the propensity of a denitrifying community to emit N_2O, but the search for evidence has not been successful (6). Genome

72 analyses show that approximately 70% of all genomes with *nosZ* also carry the genes for
73 NIR and NOR, thus regulation of denitrification in these organisms will play an important
74 role in controlling N_2O emission.

75 Regulatory networks controlling the transcription of denitrification genes have been
76 established for a number of organisms (7, 8). A common feature is the role of oxygen as a
77 superordinate repressor. This is likely a strong fitness trait because oxygen respiration is
78 energetically favorable over denitrification in terms of the generation of proton motive
79 force per electron transferred (9). Organisms in soils, biofilms and sediments are
80 frequently challenged by fluctuating O_2 concentrations and anoxic spells of variable length
81 (10). When confronted with oxygen depletion, they must synthesize a minimum
82 complement of denitrification enzymes "in time", i.e. before oxygen is completely depleted,
83 to avoid entrapment in anoxia without sufficient energy to produce a viable denitrification
84 respiratory chain (11, 12). Synthesis of the entire denitrification proteome would be a
85 waste of energy if oxygen reappears within hours. Thus, they have a regulatory dilemma,
86 which has its parallel in any organism that is forced by substrate depletion to synthesize
87 new enzymes. This was modelled by Chu (13), who concluded that leaky repression is an
88 optimal adaptation. In the case of denitrification, this would mean a leaky oxygen-
89 repression of at least one denitrification gene.

90 Experiments with *Paracoccus denitrificans* have provided some kinetic evidence for
91 leaky repression of NAR- and NOS-, but not of NIR- and NOR-, synthesis (14). Moreover, *P.*
92 *denitrificans* displays a depression of respiratory electron flow in response to oxygen
93 depletion, and this *diauxie* suggested that only a fraction of the cells synthesize active NIR
94 in time. Modelling provides support to the hypothesis that the phenomenon could be
95 ascribed to a low probability for the initiation of *nirS* transcription, but with a positive

feedback via NO and the NO sensor NnrR (12). Inspired by the fact that a similar *diauxie* in the transition from aerobic to anaerobic respiration is observed in other denitrifying organisms (12, 15), we have investigated the mechanisms in more detail in *P. denitrificans*, using a chromosomal *mCherry-NirS* fusion to track NirS, and immuno-cytostaining to track NOS synthesis and localisation in bacterial cell populations. We decided to focus on these two enzymes because: 1) As homo-dimeric soluble periplasmic proteins they are experimentally more tractable than the hetero-oligomeric integral membrane complexes NAR and NOR; 2) NIR defines the denitrification process as it performs the conversion of an aqueous N-oxyanion, nitrite, to a gaseous N-oxide, nitric oxide; and 3) NOS defines the destruction of a potent greenhouse gas which is an obligate intermediate in the full denitrification process.

Results

Many studies investigating the regulation of denitrification have focused on gene transcription, despite active enzymes being products of gene transcription, translation and post-translational modification. To enable tracking of NIR, we constructed a strain where *nirS* was replaced by a chimeric *mCherry-nirS* fusion gene under the control of the native promoter (*SI Appendix*, section 1.2), allowing visualisation of NirS-positive cells by red fluorescence. We established that mCherry-NirS fusion proteins were correctly located in the periplasm (*SI Appendix,* Fig. S15) and active confirming correct post-translational localization and cofactor insertion. The phenotype of the mCherry-NirS strain with respect to specific rate of oxygen consumption, aerobic growth rate, oxygen concentration at which denitrification is initiated and anaerobic growth rate were practically identical to the parent strain (*SI Appendix*, Table S2). Estimating the apparent probability for cells to

synthesize NirS (12) showed that (Fig. *2*): 1) the denitrification phenotype of the mCherry-NirS construct is very similar to the wild-type at all temperatures tested; 2) the apparent probability for NirS synthesis (r) increases with temperature for both strains, as predicted by the Arrhenius equation ($V=A*e^{-Ea/RT}$) with high apparent activation energy; and 3) the NO concentration-maximum increases with temperature for both strains.

To detect NOS in single cells, we developed an immunofluorescence staining method (*SI Appendix,* 1.3, Fig. S2). To differentiate between growing and non-growing cells, we tried a number of published methods, either by positive staining of growing cells, or by detecting growth as a dilution of stain, but established methods were unsuccessful for *P. denitrificans* under our experimental conditions, and we decided to design our own method (*SI Appendix*, section 1.4) *Fluorescein Isothiocyanate Cell Tracking* (FITCT). In short, cells are exposed for 10 minutes to fluorescein isothiocyanate and, after removal of excess stain, inoculated into fresh medium and their growth monitored (*SI Appendix,* 1.4). The staining was found to have negligible effects on the phenotype with respect to aerobic and anaerobic respiration and growth (*SI Appendix*, Table S2) and the fluorescence of cells was reduced by 50% for each cell division, while non-growing cells retained the fluorescence (*SI Appendix*, Fig. S9&10).

These tools allowed us to stringently test the hypothesized cell diversification summarized in Fig. *1*. Stochastic initiation of NirS transcription, leading to two subpopulations was verified by the observed fraction of red fluorescent, i.e. mCherry-NirS-positive, cells throughout batch cultivation at 17 ^{o}C (Fig. *3*). The fraction of red fluorescent cells increased as predicted by the model, which assumes a low probability for the initiation of *nirS* transcription once the repression by oxygen is relieved, and that the NirS

positive cells grow exponentially throughout the anoxic phase. Moreover, the immunocytostaining of NOS demonstrated that all cells synthesized N_2O reductase (Fig. *3*).

We also used FITCT to investigate the anaerobic growth of cells with and without NirS. These experiments were conducted with 10% acetylene to inhibit NOS (for details, see *SI Appendix,* 2.2). The results demonstrated that the FITC fluorescence was reduced gradually in the cells with NirS (red fluorescence), while the cells that lacked NirS (Fig. *4*) retained a strong FITC fluorescence. In theory, if not inhibited by acetylene, the cells without NirS (but with NOS) would be able to grow slowly by reducing N_2O provided by the cells with NirS. We have no FITC-based evidence for this, but the N_2O kinetics provide compelling evidence (12), and an experiment with N_2O in anoxic vials with nitrate/nitrite free medium demonstrated the potential for growth by N_2O as the sole electron acceptor (*SI Appendix*, Fig. S8-10).

Our model (12) assumed stochastic initiation of *nirS* transcription, with a very low probability, which then turns autocatalytic by NO via the NO-sensor NnrR. In theory, this could imply that NO produced by the first few cells carrying active NirS would induce *nirS* transcription in the rest of the population, but this is evidently not the case. A tentative explanation is that the bulk concentrations of NO are too low (10-30 nM in the liquid), due to the high-affinity NO-reductase present within actively denitrifying cells (16). A crude test of this was conducted by injecting NO to the culture at the time of oxygen depletion. The result was that nearly 100% of cells synthesized NirS and nitrite reduction to N_2 was much faster than in the control vials without NO exposure (*SI Appendix*, Fig. S17). Another prediction of the model is that in the absence of any usable electron acceptor, no cells would be able to synthesise NIR due to lack of metabolic energy; hence NIR-free cells would be entrapped in anoxia even in the presence of nitrite. However, if provided with

N_2O, they would have the energy to synthesis NIR, even in the absence of nitrogen oxyanions, albeit to a very low level due to lack of the positive regulatory feedback loop via NO and NnrR to promote synthesis of the full denitrification enzyme pathway. To explore this further, we used aerobically raised FITC-stained *mCherry-nirS* cells to inoculate anoxic vials with growth medium that was effectively stripped for nitrogen oxyanions (see (17)), and cultures were provided with N_2O as the only electron acceptor. Controls without N_2O were also included. The results demonstrated that practically all cells were able to grow by reducing N_2O, as evidenced by dilution of the FITC-fluorescence, while cells not provided with N_2O did not (*SI Appendix*, Fig. S8-10). The cells provided solely with N_2O synthesised NirS, but only to a level 1-2 orders of magnitude lower than in fully-active denitrifying cells. However, when nitrite was injected after growth on N_2O for 45 hours, NirS was synthesized to high levels in all cells. This contrasts the results for the transition from oxic to anoxic conditions, where only a low fraction of cells synthesized NirS. It could be taken to suggest a regulatory effect of prolonged exposure to anoxia and N_2O as the sole electron acceptor, enabling all the cells to synthesize NirS when provided with nitrite. To our knowledge, no regulatory effect of N_2O on denitrification has been proven (18).

Fate of denitrification enzymes during oxic spells

Little is known about the fate of the denitrification enzymes once oxygen returns. They could either be diluted by aerobic growth, degraded, or localized in ageing cells by asymmetric distribution among daughter cells, as has been demonstrated both with cytoplasmic (19, 20) and periplasmic proteins (21). As a first approach to investigate the fate of the denitrification proteome, we designed an "entrapment assay" in which cells without intact NIR would be unable to grow: the cell suspensions to be tested were

transferred to anoxic media without nitrogen oxyanions, to which nitrite was added after depletion of the last traces of oxygen. Cells without NIR (raised through >10 generations of aerobic growth) were unable to initiate anaerobic respiration, while cells with NIR (anaerobically raised cells) were active immediately. We used this assay to assess the fate of a denitrification proteome during aerobic growth. *P. denitrificans* was raised by >12 generations of anaerobic growth on nitrite, ensuring that all cells carried a full set of denitrification enzymes. These denitrifying cultures were then exposed to fully oxic conditions in medium without nitrogen oxyanions and allowed to grow by aerobic respiration up to ~12 generations. At intervals cells were tested with the entrapment assay (*SI Appendix*, Fig. S3) using the kinetics of nitrite reduction to N_2 to assess the fraction of Entrapment Assay Competent cells (EAC) i.e. cells that were able to initiate anaerobic respiration and growth in this assay.

The experiment had three alternative outcomes: 1) If cells actively degrade NIR, we would observe a rapid decline in EAC throughout the first generations of aerobic growth; 2) If NIR is not actively degraded, but evenly distributed among daughter cells, the fraction of EAC would remain constant throughout the first generations of aerobic growth until the NIR content reached a critically low concentration (diluted by growth); 3) if NIR is not actively degraded, but localized to the old poles of the cells during aerobic growth, the fraction of EAC would decline by 50% for each generation of aerobic growth. The result (Fig. *5*) suggested the latter. Here, the number of EAC per mL remained practically constant throughout 12 generations of aerobic growth (Fig. *5B*), resulting in a gradual decline in percent EAC as predicted (Fig. *5C*).

Preferential localization of certain virulence proteins at the old cell poles has been established previously in *Shigella flexneri* (21). In order to examine the nature of NirS

localization and distribution in pure-cultures of *P. denitrificans* further, time lapse microscopy of anaerobically raised cells was performed during aerobic growth on agar pads. Here, the following patterns were observed (Fig. *6*): In practically all cells, mCherry-NirS migrated to the cell poles within minutes after exposure to oxygen (*SI Appendix*, Movie SV1). Some cells did not grow at all, and for this cell population NirS remained at the poles (*SI Appendix*, Movie SV2). The cells that did grow, first redistributed their NirS to the entire periplasm, and started to grow, diluting their NirS by even distribution among daughter cells (Figs. *6* and *SI Appendix*, Fig. S16 and Movie SV3). However, some cells within micro-colonies of growing cells stopped growing after 1-3 generations, and in these cells, NirS migrated back to the poles (Fig. *6B-D*, *SI Appendix,* Movie SV4).

This pattern provides a plausible explanation to the observed result of the entrapment assay: the arrested growth by some of the cells qualifies for the term *persister cells*, because they are cells that retain their NirS in a potentially active form, hence enabling them to tackle sudden anoxia. Conversely, the cells that became engaged in aerobic respiration and thereby diluted their NirS pool, lost the ability to switch to anaerobic respiration in the entrapment assay.

Control experiments were conducted to exclude artifacts regarding the migration of NirS to the cell pole. A strain with inducible expression of *mCherry* that was transported to the periplasm was constructed (SI *Appendix*, 1.2.2), and growth experiments demonstrated even distribution of mCherry throughout the periplasm and no migration to the cell pole in response to oxygen was observed (*SI Appendix*, Fig. S11). Thus, the migration of mCherry-NirS to the cell pole in response to oxygen is clearly due to a property of NirS, not mCherry. In addition, cells inactivated by NaN_3 showed no migration to the pole (*SI Appendix*, Fig. S12), hence the migration depends on some metabolic integrity. To exclude artifacts

created by the agar pad conditions, we corroborated the polar localization by transferring anaerobically grown cells to aerobic vials which were sampled for microscopy (fixed by formalin immediately after sampling). Samples taken throughout the first 30 minutes confirmed rapid migration to the poles, and samples taken after 2-5 generations of aerobic growth demonstrated that the *persister cells* had NirS localized at the cell poles. We also observed migration to the cell poles under anoxic conditions, but only in response to depletion of electron acceptors (*SI Appendix*, Fig. S13).

Discussion

Cell diversification in isogenic cultures has been described in a wide variety of prokaryotes, and the phenomenon is ascribed to noise and bistability of the regulatory networks (22, 23). Well-documented cases are endospore formation, chemotaxis, expression of genes for substrate utilization (*lac* operon in *E. coli*), and the formation of *persister cells* (24). Some such phenomena are termed *bet-hedging* because the population spreads the risks when responding to fluctuating conditions; in effect accepting a penalty for a fraction of the population, in exchange for a long-term fitness advantage for the entire population (25).

This present study reveals that *P. denitrificans* cells display a bet-hedging strategy with respect to the synthesis of NIR when challenged with imminent anoxia. Most likely, the synthesis of NOR is coordinated with NIR, as indicated by the NO kinetics during denitrification (16). The hypothesized mechanism was a constant, low probability of initial *nirS* transcription, but with a positive feedback loop via NO and NnrR (12, 26), and this is supported by our experimental results. Moreover, we observed a strong effect of temperature on the probability for NirS-synthesis (Fig. *2*). The probability of expressing the

entire denitrification proteome increased sharply with temperature, resulting in pronounced bet hedging at low temperatures, while a high fraction of the cells express the entire denitrification proteome at high temperature. This would make sense if the probability of severe/long-lasting anoxic spells increase with increasing soil temperature (since this would penalize the cells without NIR+NOR). This is indeed plausible if we think of anoxic spells induced by transient waterlogging of soil (after heavy rain): The oxygen consumption rate will increase with temperature, while the rate of drainage (thus restoring oxic conditions) will not. Hence, the probability of severe/long anoxic spells would increase with increasing temperature. The temperature effect explains why the bet-hedging phenomenon has gone undiscovered until now because, in general, *P. denitrificans* has been studied at temperatures ≥ 30°C wherein the phenomenon is almost undetectable (Fig. *2A*). This underscores the importance of conducting physiological experiments under environmentally relevant conditions.

The regulation of NIR-synthesis in *P. denitrificans* can be seen as a beneficial energy-conserving strategy, i.e. minimizing the cost of protein synthesis in all cases when oxygen quickly reappears to adapt to changing environmental conditions. It could prove fatal, however, if it results in complete entrapment of the majority of cells in long-term anoxia. This penalty is evidently avoided by a leaky repression of *nosZ* (and possibly *nar*). By synthesizing NOS in 100% of the population in response to hypoxic conditions, *P. denitrificans* ensures continued respiratory growth, albeit slow, by scavenging N_2O produced by other cells in the population or the community. Should the anoxic spell be prolonged, these cells will eventually synthesize active NIR using the energy conserved from N_2O respiration (*SI Appendix*, Fig. S9). Thus, *P. denitrificans* can be predicted to act as a strong N_2O sink in temperate environments with frequent fluctuations in O_2 availability.

As such, our observations have environmental implications as several denitrifying bacteria have displayed *diauxie* during transition from oxic to anoxic conditions (refs in (12, 26)) and a number of newly isolated strains from soil displayed a clear depression of the respiratory electron flow during the transition from oxic to anoxic conditions (15).

An important question is how does bet-hedging contribute to the survival of the population? The entrapment assay demonstrates that organisms can become entrapped in anoxia if exposed to sudden disappearance of oxygen. This is possibly a rare phenomenon in natural environments, however, where most anoxic spells are plausibly initiated by a more gradual depletion of oxygen. Thus, the advantage of bet-hedging would primarily be to save energy by synthesizing only NAR and NOS in the majority of cells. NOS could possibly provide better protection against entrapment than NAR, since nitrate depletion is a more likely event than N_2O depletion. N_2O will probably linger longer, albeit at low concentrations, for two reasons: 1) it is the last intermediate in the sequential reduction of nitrate to N_2, hence traces will be left after the reduction of the last molecule of nitrate (14) and 2) N_2O will be produced in hypoxic/oxic fractions of the soil matrix, both by nitrification and denitrification, and transported to the anoxic sites. This is corroborated by measurements of N_2O concentrations in soil atmosphere, which are almost invariably higher than ambient concentrations (32). Arguably, traces of nitrate will remain in the soil matrix as well (produced in hypoxic/oxic fractions of the matrix), but the transport of nitrate within the soil matrix is much slower than that of N_2O (transport by diffusion in water is slower than in the gas phase).

We have demonstrated spatiotemporal variation of NirS localization in *P. denitrificans* (Fig. *6*, *SI Appendix* Movie SV1-4), which was evenly distributed during anaerobic growth, but migrated to the poles in response to depletion of electron acceptors,

311 and if cells were transferred to oxic conditions. Subcellular localization of cytoplasmic
312 proteins has been described in a range of bacteria, and it is evident that the organisation of
313 proteins is subject to spatiotemporal regulation. Polar localization of proteins serves a
314 number of purposes and is involved in asymmetric cell division, modulation of the cell
315 cycle, chemotaxis and motility (27), and shedding of useless/damaged proteins (28). A
316 number of mechanisms governing polar localization of proteins in the cytoplasm have been
317 described (29). However, only a few examples of spatially organised periplasmic proteins
318 have been reported (21). Spatiotemporal organization of cytoplasmic proteins is often
319 intimately linked to cell cycle and proton motive force (30), and it is reasonable to assume
320 that periplasmic enzymes associating with the membrane or membrane bound factors, may
321 be governed by similar rules. The activity of NirS is linked to a range of factors and it makes
322 little sense for the enzyme to exist as a detached entity floating freely in the periplasm. On
323 the contrary, it is likely to interact intimately with the other denitrification enzymes, such
324 as the membrane embedded NorBC during active denitrification (31). Membrane
325 associated factors may in turn interact with cytoplasmic proteins in a manner dependent
326 on the electrogenic state of the membrane. In this scenario, NOR and NirS may engage in a
327 "capture and release" cycle driven by the proton motive force. Once detached from NOR,
328 NirS may diffuse passively to the poles and/or interact with a secondary partner with polar
329 localization. Alternatively, and perhaps more likely, NirS may migrate in complex with its
330 membrane-embedded partners in a manner dependent on their interaction with the
331 cytoplasm. A link between the proton motive force and NirS localization is supported by
332 the observation of migration of NirS to the cell poles under anoxic conditions in response to
333 exhaustion of NO_x (*SI Appendix*, Fig. S13). In contrast, there was no evidence of migration of
334 NOS to the cell pole under any of the conditions tested (Fig. *3*, *SI Appendix*, Fig. S14). NosZ

335 may form a complex with the integral membrane protein NosR rather than NorBC (31),
336 which could explain the divergent localization response of NosZ and NirS.

337 Much like rapid transitions from aerobic to anaerobic growth, the abrupt return of
338 oxygen in the absence of N-oxides can be viewed as a crisis with profound regulatory
339 challenges. In order to grow, cells must reassemble their aerobic respirome, and this may
340 require *de novo* protein synthesis dependent on existing energy reserves. Thus, the
341 conservation of NIR in non-growing persister cells, may be a result of energy depletion, i.e.
342 "entrapment in oxia" in a select fraction of cells fully invested in an anaerobic lifestyle. We
343 can only speculate as to the mechanisms involved in the formation of persister cells at this
344 point, and more work is needed in order to verify their actual role in persistence of NIR
345 during oxic spells.

346

347 **Conclusion**

348 Bet-hedging with respect to NIR, coupled with early and complete onset of NOS, bear
349 environmental implications because organisms with this regulatory set-up become strong
350 net sinks of N_2O. Moreover, at the risk of unduly anthropomorphizing non-sentient
351 organisms, such phenotypic heterogeneity can be seen as an ingenious strategy for
352 safeguarding ones interests without exhaustive investments. Placing wagers on multiple
353 near-future outcomes nullifies the risk on population level, at lower costs than full
354 synthesis of all enzymes.

355

356 **Materials and methods**

357 Batch cultivation, monitoring of gas kinetics, and modelling of recruitment to anaerobic
358 respiration during oxygen depletion is described in *SI Appendix* 1.1. The construction of the

mCherry-NirS strain, and the control strain with naked periplasmic mCherry is described in *SI Appendix* 1.2. The development of immunocytostaining of NOS is described in *SI Appendix* 1.3. Development of the FITC method and the testing of phenotypic effects of the staining is described in *SI Appendix* 1.4 and 2.3. Fluorescence microscopy and time lapse imaging of cells on agar slabs is described in *SI Appendix* 1.5. The entrapment assay, designed to assess the number of cells that are able to switch to anaerobic respiration in response to sudden anoxia is described in *SI Appendix* 1.6.

Acknowledgements

P Lycus and MJ Soriano-Laguna were financed by NORA MCS ITN from the EU 7th Framework Programme under Grant agreement no 316472. AJ Gates acknowledges support from the Biotechnology and Biological Sciences Research Council, U.K. (Grant Ref. BB/M00256X/1). L Bergaust was financed by Research Council of Norway (Grants 231282/F20 and 275389/F20).

References

1. Galloway JN *et al.* (2004) Nitrogen cycles: past, present and future. *Biogeochemistry* 70:153-226.
2. Schlesinger WH (2009). On the fate of anthropogenic nitrogen. *Proc Natl Acad Sci USA* 106(1):203-208.
3. Ravishankara AR, Daniel JS, Portmann RW (2009) Nitrous oxide (N_2O): the dominant ozone-depleting substance emitted in the 21st century. *Science* 326: 123–125 doi: 10.1126/science.1176985

4. Shapleigh JP (2013) Denitrifying Prokaryotes. In: Rosenberg E, DeLong EF, Lory S, Stackebrandt E, Thompson F (eds) The Prokaryotes. Springer, Berlin, Heidelberg
5. Graf DRH, Jones CM, Hallin S (2014) Intergenomic Comparisons Highlight Modularity of the Denitrification Pathway and Underpin the Importance of Community Structure for N_2O Emissions. PLoS ONE 9(12): e114118. doi:10.1371/journal.pone.0114118
6. Bakken LR, Frostegård Å (2017) Sources and sinks for N_2O, can microbiologists help to mitigate N_2O emissions? *Environ Microbiol* 19:4801-4805.
7. Van Spanning RJM, Richardson DJ, Ferguson S (2007) Introduction to the biochemistry and molecular biology of denitrification. p 3-21 in: Bothe H, Ferguson S, Newton WE (eds) The biology of the Nitrogen cycle. Elsevier (Amsterdam) ISBN-13: 978-0-444-52857-5.
8. Zumft WG, Kroneck P (2007) Respiratory transformation of nitrous oxide (N_2O) to dinitrogen by Bacteria and Archaea. *Adv Microb Physiol* 52:107- 227.
9. Chen J, Strous M (2013) Denitrification and aerobic respiration, hybrid electron transport chains and co-evolution. *BBA* 1827:136-144.
10. Marchant HK *et al.* (2017) Denitrifying community in costal sediments performs aerobic and anaerobic respiration simultaneously. *ISME J* 11:1799-1812.
11. Højberg O, Binnerup SJ, Sørensen J (1997) Growth of silicone-immobilized bacteria cells on polycarbonate membrane filters, a technique to study

405 microcolony formation under anaerobic conditions. *Appl Environ Microbiol*
406 63:2920–2924.
407 12. Hassan J, Qu Z, Bergaust LL, Bakken LR (2016) Transient Accumulation of
408 NO_2^- and N_2O during Denitrification Explained by Assuming Cell
409 Diversification by Stochastic Transcription of Denitrification Genes. *PLoS*
410 *Comput Biol* 12(1):e1004621.
411 13. Chu D (2017) Limited by sensing – A minimal stochastic model or the lag-
412 phase during diauxic growth. *J Theor Biol* 414:137-146.
413 14. Qu Z, Bakken LR, Molstad L, Frostegård Å, Bergaust LL (2016) Transcriptional
414 and metabolic regulation of denitrification in *Paracoccus denitrificans* allows
415 low but significant activity of nitrous oxide reductase under oxic conditions.
416 *Environ Microbiol* 18(9):2951-2963.
417 15. Lycus P *et al.* (2017) Phenotypic and genotypic richness of denitrifiers
418 revealed by a novel isolation strategy. *ISME J* 11:2219-2232.
419 16. Hassan J, Bergaust L, Molstad L, deVries S, Bakken LR (2016) Homeostatic
420 control of nitric oxide (NO) at nanomolar concentrations in denitrifying
421 bacteria – modelling and experimental determination of NO reductase
422 kinetics *in vivo* in *Paracoccus denitrificans*. *Environ Microbiol* 18:2964-2978.
423 17. Bergaust L, van Spanning RJM, Frostegård Å, Bakken LR (2012) Expression of
424 nitrous oxide reductase in *Paracoccus denitrificans* is regulated by oxygen and
425 nitric oxide through FnrP and NNR. *Microbiology* 158:826-834.
426 18. Sullivan MJ, Gates AJ, Appia-Ayme C, Rowley G, Richardson DJ (2013) Copper
427 control of bacterial nitrous oxide emission and its impact on vitamin B12-
428 dependent metabolism. *Proc Natl Acad Sci USA* 110(49):19926-19931.

19. Lindner AB, Madden R, Demarez A, Stewart EJ, Taddei F (2008) Assymetric segregation of protein aggregates is associated with cellular aging and rejuvenation. *Proc Natl Acad Sci USA* 105:3076-3081.
20. Macara IG, Mili S (2008) Polarity and differential inheritance – universal attributes of life? *Cell* 135: 801-812
21. Scribano D *et al.* (2014) Polar localization of PhoN2, a periplasmic virulence-associated factor of *Shigella flexneri*, is required for proper IcsA exposition at the old bacterial pole. *PLoS ONE* 9(2): e90230. doi:10.1371/journal.pone.0090230
22. Ackermann M (2013) Microbial individuality in the natural environment. *ISME J* 7:465-467.
23. Veening JW, Smits WK, Kuipers OP (2008) Bistability, epigenetics, and bet-hedging in bacteria. *Ann Rev Microbiol* 62:193–210.
24. Lewis K (2007) Persister cells, dormancy and infectious disease. *Nat Rev* 5:48-56.
25. de Jong IG, Haccou P, Kuipers OP (2011) Bet hedging or not? A guide to proper classification of microbial survival strategies. *Bioessays* 33(3):215-223.
26. Hassan J, Bergaust LL, Wheat ID, Bakken LR (2014) Low probability of initiating *nirS* transcription explains observed gas kinetics and growth of bacteria switching from aerobic respiration to denitrification. *PLoS Comput Biol* 10(11): e1003933.
27. Davis BM, Waldor MK (2013) Establishing polar identity in gram-negative rods. *Curr Opin Microbiol* 16(6):752-759.

28. Tyedmers J, Mogk A, Bukau B (2010) Cellular strategies for controlling protein aggregation. *Nat Rev* 11:777-788.

29. Laloux G, Jacobs-Wagner C (2014) How do bacteria localize proteins to the cell pole? *J Cell Sci* 127(1):11-19.

30. Strahl H, Hamoen LW (2010). Membrane potential is important for bacterial cell division. *Proc Natl Acad Sci USA* 107(27):12281-12286.

31. Borrero-de Acuña JM *et al.* (2016) Protein network of the *Pseudomonas aeruginosa* denitrification apparatus. *J Bacteriol* 198(9):1401-1413.

32. Flechard CR, Neftel A, Jocher M, Ammann C, Fuhrer J (2005) Bi-directional soil/atmosphere N_2O exchange over two mown grassland systems with contrasting management practices. *Global Change Biology* 11: 2114–2127

Figure legends

Fig. 1. Hypothesized cell diversification of *P. denitrificans* in response to oxygen depletion, corroborated by modelling the diauxic electron flow kinetics (Fig *2*). The model assumptions are that all cells synthesize NOS, while NAR and NIR+NOR synthesis is stochastic; occurring with a specific probability which is moderate for NAR (0.03-0.04 h^{-1}), very low for NIR+NOR (~0.004 h^{-1}), but with a positive feedback via NO (12)). The different probabilities for a cell to synthesize NAR and NIR+NOR implies that after 30 hours with critically low oxygen concentrations, 70-77% of the cells have synthesized NAR, while only 11% of the cells have synthesized NIR+NOR. Cells without NIR (but with NOS) can respire by reducing the N_2O produced by the cells with NIR. Thus, the entire population effectively avoids entrapment in anoxia.

Fig. 2. Denitrification phenotype of the *mCherry-NirS* strain and the wild type as a function of temperature. The A panels show gas- and electron flow kinetics, measured and modelled (model: Hassan *et al*. (12)) for single vials (wild type) at the two extreme temperatures tested; 30 and 17 ^{o}C. The characteristic depression in electron flow rate after oxygen depletion at 17 ^{o}C is hardly detectable at 30 ^{o}C. The experiment was performed with 3-6 replicate vials at different temperatures, and the probability for initiation of NirS transcription (r, h^{-1}) was estimated for each individual vial, and ln(r) plotted against the inverse temperature (K^{-1}, Panel B, bottom), showing reasonably linear decline (wild type: y=64.38-20113x; R^2=0.9549 and mCherry-NirS strain: y=41.95-13396x; R^2=0.8904). The estimated apparent activation energy is 111 (se 26) and 166 (se 35) kJ mol^{-1} for the *mCherry-NirS* strain and the wild type, respectively ($p<0.01$ for the difference between strains). The maximum NO concentrations at the different temperatures (nM NO) is shown in the top B panel. The entire dataset and the model fits are shown in *SI Appendix*, Fig. S4&5.

Figure 3: Gas kinetics and synthesis of NirS and NosZ in Pd1222 carrying *mCherry-NirS* during the transition from aerobic respiration to denitrification (17 ^{o}C). Panel A shows the depletion of O_2 followed by accumulation of NO and recovery of the initial 2 mM NO_2^--N (= 100 µmol N $vial^{-1}$) as N_2. N_2O was in the low nanomolar range throughout the incubation. Panel C shows microscopic images of cells immunocytostained for NosZ, taken at the time of oxygen depletion (42 h, upper row) and at depletion of e^- acceptors (70 h, lower row). The images (panel C), from left to right, show the mCherry fluorescence (mC), NOS immunofluorescence (NosZ), and phase contrast (PC). Scale bar is 2 µm. All cells stained

positive for NOS at the time of transition, while none were positive for NirS. In the late sample (70 h), all cells stained positive for N_2O reductase and a high fraction showed mCherry-NirS fluorescence. Several samples were taken at different times throughout the anoxic phase, and the fraction of mCherry-NirS positive cells were enumerated. Panel B shows the recorded frequencies of mCherry-NirS positive cells (as defined in Fig. *4*), plotted against the model predictions for two experiments in which aerobically raised cells were inoculated to near-anoxic vials with 10% acetylene (red circles, see Fig. *4* for further details) and without acetylene (blue, see *SI Appendix, Fig*. S7 for further details).

Fig. 4: Anaerobic growth by the subpopulation with NirS, visualized by FITC stained cells of the *mCherry-NirS* strain. Cells stained with FITC were transferred to near-anaerobic vials with Sistrom's medium (2 mM NO_2^-) and 10 % acetylene in the headspace. Panel A shows gas kinetics (N_2O measurement as red squares and model as black line), inserted panel: observed frequency of mCherry-NirS positive cells (fluorescence>250) with the modelled frequency (black line). Panel B shows micrographs of cells after 48 h; same frame in all four squares (FITC-fluorescence, mCherry fluorescence (mC), phase contrast (PC) and a combination of all). Panel C shows single cell fluorescence distribution throughout the anaerobic incubation. The crossed lines show the average and standard deviation of the fluorescence intensity for two populations: red cross for cells with mC>500, green cross for cells with mC<500. For better resolution regarding the low mCherry fluorescence, see log plots of the same data in *SI Appendix*, Fig. S6.

Fig. 5. Fate of denitrification proteome during aerobic growth. Anaerobically raised cells were grown aerobically, and after 1-12 generations they were tested for their ability to switch to anaerobic respiration in the Entrapment Assay (sudden anoxia, ensuring that cells without NIR are effectively entrapped in anoxia). The main panel shows the electron flow to N-oxides ($Ve\text{-}_{NOx}$) during the entrapment assay for cells sampled after 0, 1, 2, 4 and 12 generations of aerobic growth (initial cell number was 10^{10} in each assay). The cumulative N_2 production is shown in insert 3 (logarithmic time scale). Continuous lines (both in the main panel and insert) show the model (12) fitted to the data (least square) by adjusting the initial number of cells that switched to anaerobic respiration and growth (EAC= Entrapment Assay Competent Cells). Insert panel 1 is a reconstruction of aerobic growth through 12 generations, plotting population size relative to initial number (N/N_0): while EAC remained essentially constant, the total number of cells increased by a factor of 4000. Insert panel 2 shows the %EAC in each sample, together with prediction (solid line), assuming asymmetric distribution of NirS during aerobic growth, i.e. that all NirS migrates to one daughter cell. These results were taken to suggest asymmetric distribution, but the time lapse imaging of aerobically growing cells provided a more plausible explanation (Fig. *6*).

Fig. 6. Time lapse photos of cells with intact NirS during aerobic growth on agar slabs. Panel A shows the time lapse of a single and a doublet cell which failed to grow aerobically and retained mCherry-NirS at the poles. Redistribution occurred in the single cell after 120 min, and it eventually divided. Panel B shows a growing cell, with even distribution of mCherry-NirS, growing fast from the very beginning. However, a single cell among the third generation cells stopped growing (indicated by arrowheads), retaining mCherry-NirS,

546 while the rest of the population continued to dilute NirS by growth. This is further
547 illustrated by the cell lineage and mCherry intensity of individual cells (see also SV4) in the
548 two lower panels. Scale bars are 2 μm. Full-frame pictures are shown in Fig. S16, and a
549 corresponding time lapse video (SV2) is available. See also time lapse movies of the
550 growing cells in panel A and C (*SI Appendix*, Movie SV3, SV4). The total fluorescence signal
551 for micro-colonies and for non-growing cells remained practically constant throughout the
552 experiment (*SI Appendix*, Fig. S18).

Denitrifying organisms sustain anaerobic respiration by the stepwise reduction of NO_3^- to N_2, catalyzed by four metallo-enzymes:

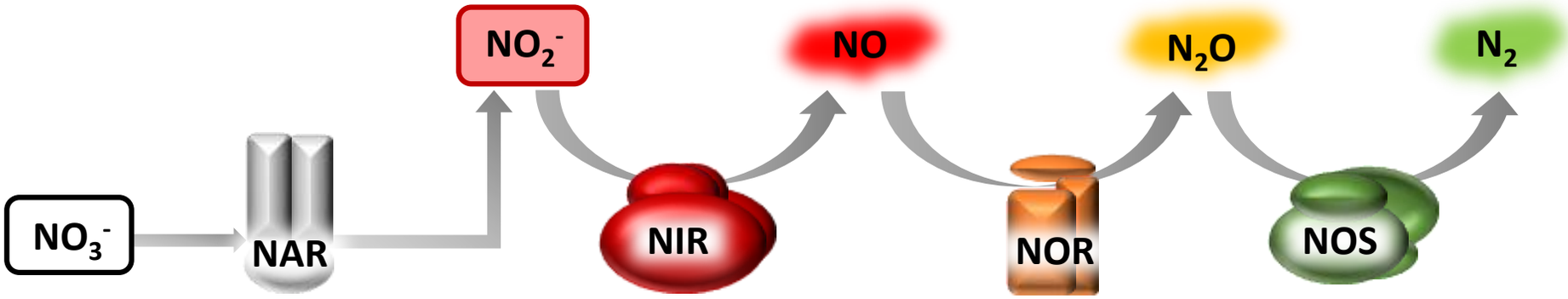

Hypothesized cell diversification in response to oxygen depletion:

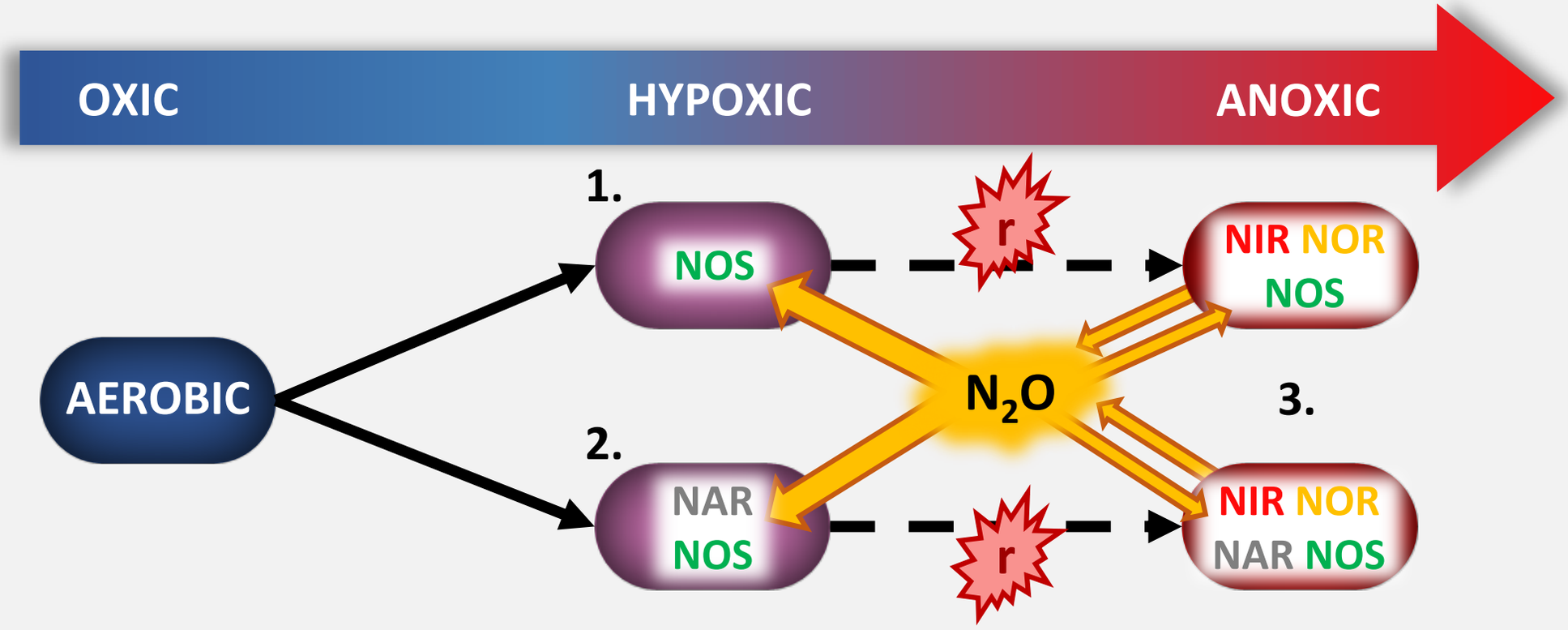

1. Early expression of **NOS** in all cells
2. Early expression of **NAR** in most cells
3. Stochastic expression of **NIR** + **NOR**, with low probability **r**, h^{-1}

Strong net sink for N_2O

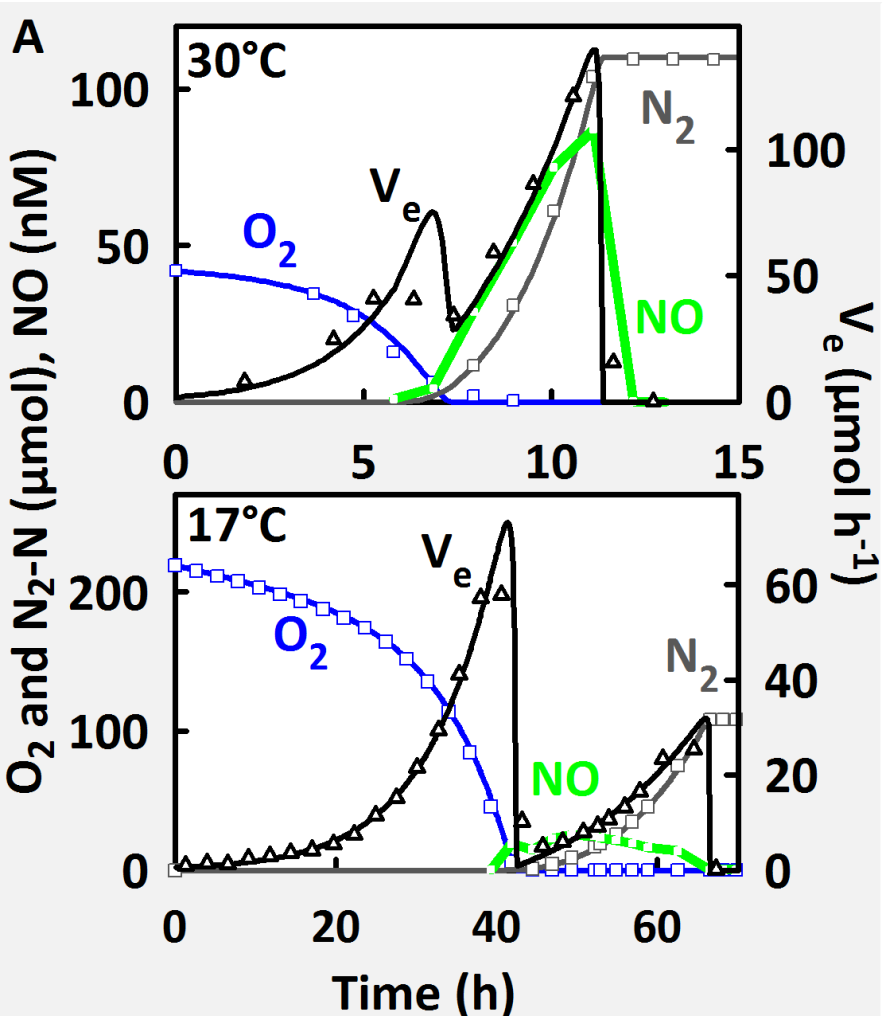
A
30°C
100
50
0
0
5
10
15
O_2
V_e
N_2
NO
17°C
200
100
0
0
20
40
60
O_2
V_e
N_2
NO
O_2 and N_2-N (µmol), NO (nM)
V_e (µmol h^{-1})
Time (h)

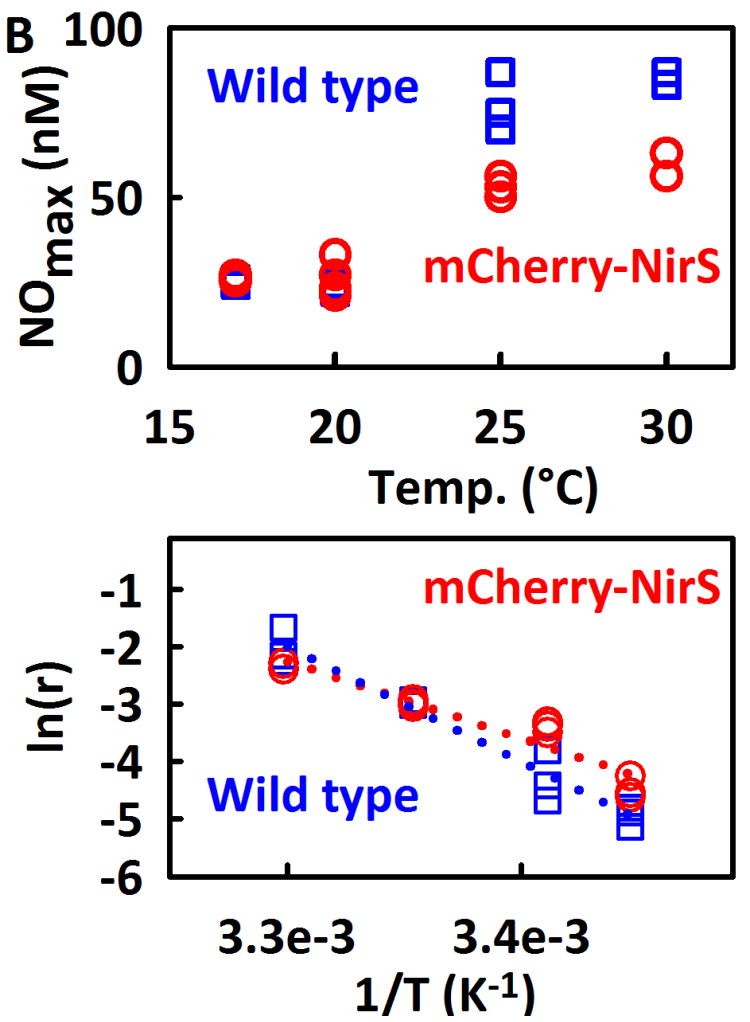
B
100
50
0
Wild type
mCherry-NirS
NO_{max} (nM)
15
20
25
30
Temp. (°C)
-1
-2
-3
-4
-5
-6
mCherry-NirS
Wild type
ln(r)
3.3e-3
3.4e-3
1/T (K^{-1})

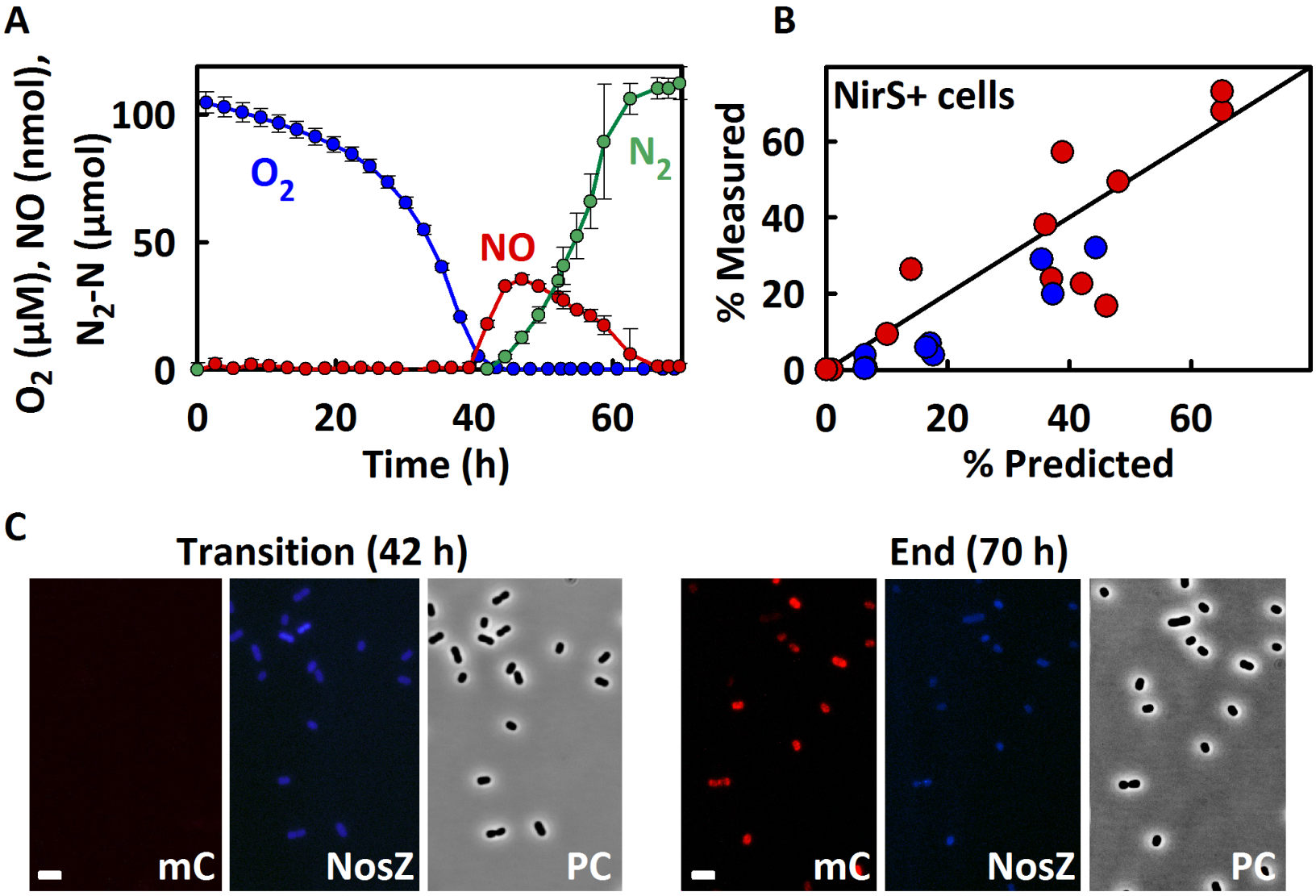
A
O_2 (µM), NO (nmol), N_2-N (µmol)
100
50
0
O_2
NO
N_2
0
20
40
60
Time (h)
B
NirS+ cells
% Measured
60
40
20
0
0
20
40
60
% Predicted
C
Transition (42 h)
End (70 h)
mC
NosZ
PC
mC
NosZ
PC

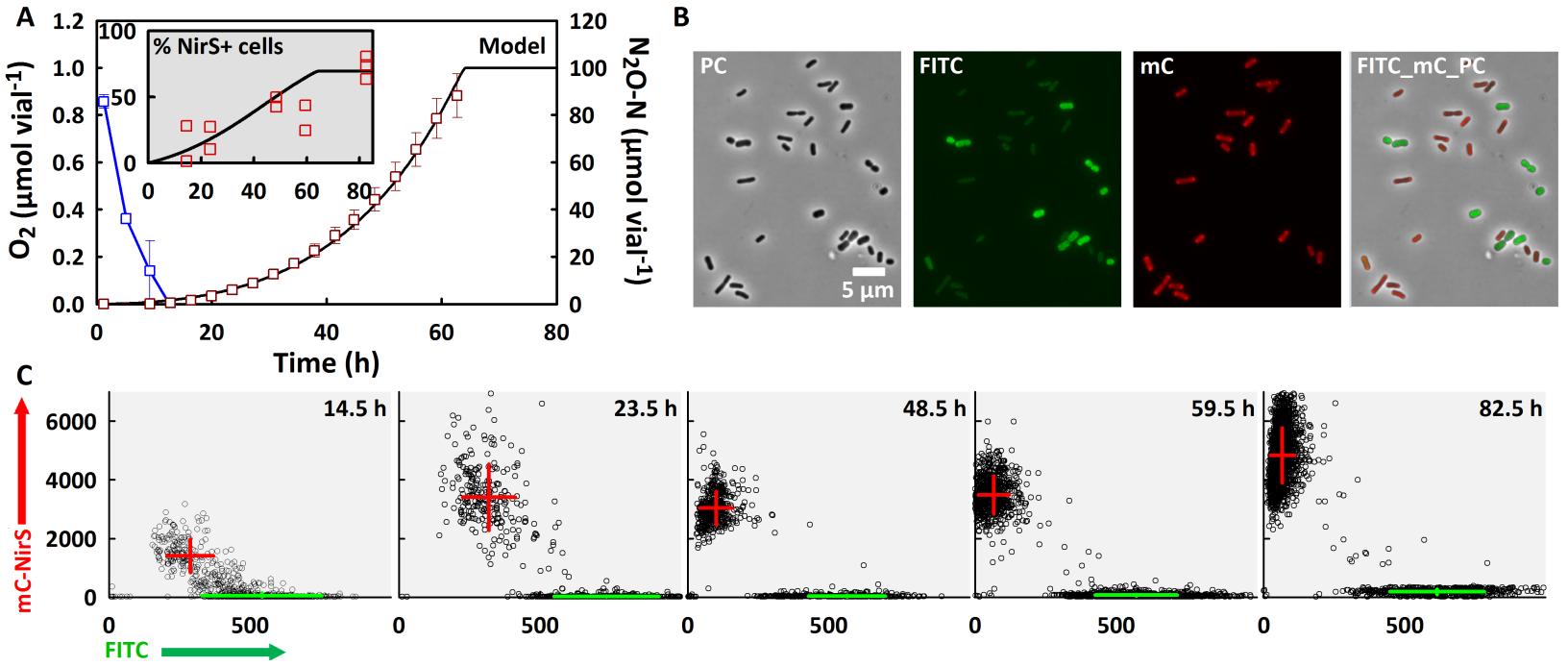
A
B
C
O_2 (µmol vial^{-1})
N_2O-N (µmol vial^{-1})
Time (h)
% NirS+ cells
Model
PC
FITC
mC
FITC_mC_PC
5 µm
mC-NirS
FITC
14.5 h
23.5 h
48.5 h
59.5 h
82.5 h

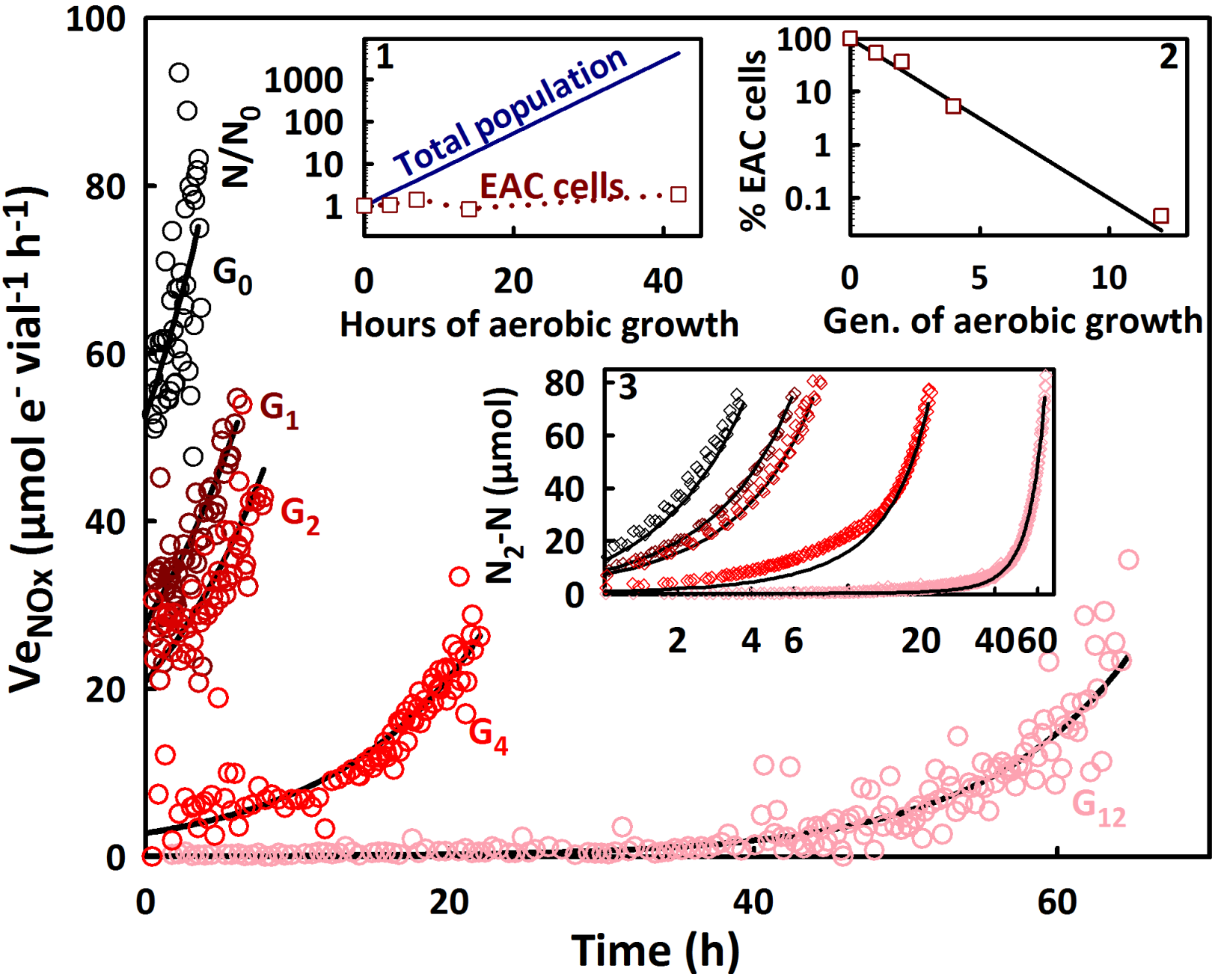
Ve$_{NOx}$ (µmol e$^-$ vial^{-1} h^{-1})
Time (h)
G$_0$
G$_1$
G$_2$
G$_4$
G$_{12}$
1
N/N$_0$
Total population
EAC cells
Hours of aerobic growth
2
% EAC cells
Gen. of aerobic growth
3
N$_2$-N (µmol)

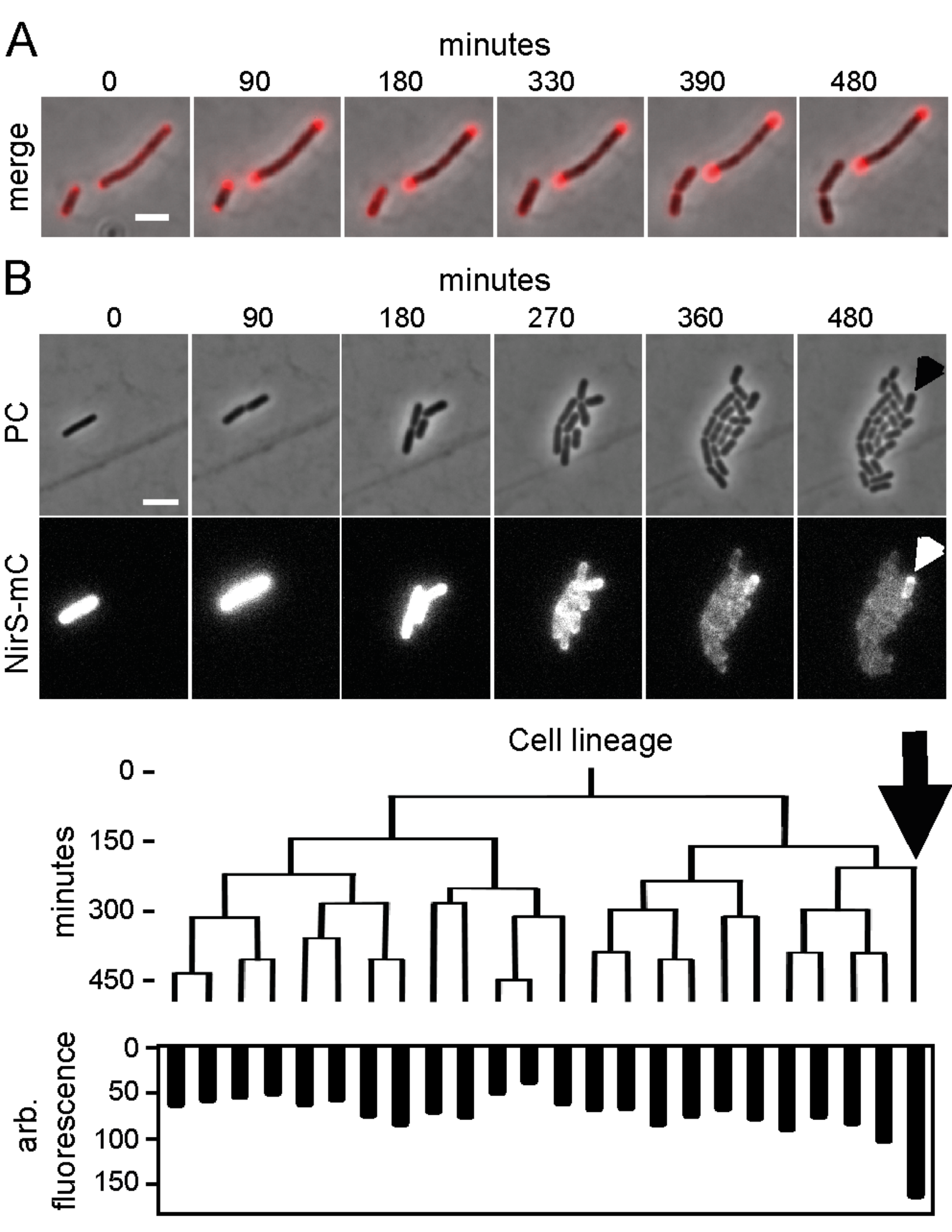
A
minutes
0
90
180
330
390
480
merge
B
minutes
0
90
180
270
360
480
PC
NirS-mC
Cell lineage
0
150
300
450
minutes
arb.
fluorescence
0
50
100
150